PROCEEDINGS, Thirty-Sixth Workshop on Geothermal Reservoir Engineering
Stanford University, Stanford, California, January 31 - February 2, 2011
SGP-TR-191

UNCERTAINTY QUANTIFICATION OF THMC PROCESSES IN FRACTURED MEDIA FOR SYSTEMS MODELING

Souheil M. Ezzedine[1,2], Ilya N. Lomov[3], Lee G. Glascoe[1], Tarabay H. Antoun[3]

[1]Lawrence Livermore National Laboratory; National Security Engineering Division, L-188
7000 East Avenue, Livermore, CA 94550; e-mail: ezzedine1@llnl.gov
[2]Stanford University, Department of Civil and Environmental Engineering,
473 Via Ortega, Y2E2 Bldg, Stanford, CA 94305
[3]Lawrence Livermore National Laboratory; National Security Engineering Division, L-286
7000 East Avenue, Livermore, CA 94550

ABSTRACT

Hybrid system modeling is an emerging field in flow and transport in porous fractured media. Known the effective behavior of an engineered system, such as geothermal system, at different scale is essential to successfully design and predict complex operational conditions. A major issue to overcome when characterizing a deep fractured reservoir is that of data limitation due to accessibility and affordability. Moreover, the ability to map discontinuities in the rock with available geological and geophysical tools tends to decrease particularly as the scale of the discontinuity goes down. Geological characterization data include, but are not limited to, measurements of fracture density, orientation, extent, and aperture. All of which are taken at the field scale through a very sparse limited number of deep boreholes. These types of data are often reduced to probability distribution functions for predictive modeling and simulation in a stochastic discrete framework. Stochastic discrete fracture network (SDFN) models enable, through Monte Carlo simulations, the probabilistic assessment of flow and transport phenomena that are not adequately captured using continuum models. Despite the fundamental uncertainties inherited within the probabilistic reduction of the sparse data collected, very little work has been conducted on quantifying uncertainty on the reduced probabilistic distribution functions. Using nested Monte Carlo simulations, we investigated the impact of parameter uncertainties of the discrete fracture network on the flow, heat and mass transport using physical characteristics such as the hydraulic conductivity tensor, production temperatures and peak arrival time.

INTRODUCTION & PROBLEM STATEMENT

The logical steps that must be taken to complete an EGS reservoir project are (Figure 1): (1) finding and characterizing a site by drilling and logging exploratory wells; (2) creating the reservoir by drilling an injection well, stimulating the fractures and drilling extraction well(s); and (3) operating the reservoir by completing and verifying the circulation loop and installing operating equipment (DOE, 2008). Despite that geothermal energy is a mature geosciences energy technology, the success of old and new approaches remain limited by the sparse knowledge gained from the geological site characterization and the fundamental uncertainties inherited within the probabilistic reduction of the sparse data collected and their adequacy for the mechanical and chemical stimulation of geothermal systems.

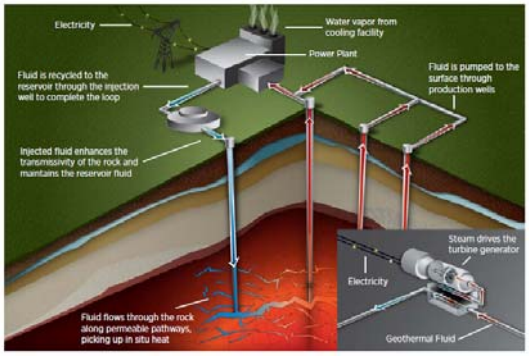

Figure 1: Logical steps to complete an EGS reservoir project (DOE, 2010)

Despite that design and predictive tools and codes (e.g. Ezzedine, 1994; Pruess, 2006; McLure, 2010) exist very limited knowledge has been gained on their applicability and validity of their assumptions. The objective of the present paper is to assess in a more comprehensive manner the impact of uncertainty associated with the geological site characterization on the flow, heat and mass transport responses of an EGS system. This objective is treated in a stochastic framework and will supplement the work of Ezzedine (2010) where only flow through a DFN system is addressed. The current uncertainty does serve two purposes. First, uncertainty within the production temperature can be fed into the surface facility design of an EGS. Second, the uncertainty

within the reacting mass transport can be fed into surface area heat exchanger estimator, thus optimal design of a topology of a fractured network system.

CONCEPTUAL MODEL OF FRACTURED MEDIA: THE DISCRETE APPROACH

Several different approaches, or concepts, have been used to describe the fractured mass (Ezzedine, 2005 and references therein). Hereafter, we focus only on stochastic DFN models which are appropriate when the characterization of deep fractured reservoirs is limited to a few sparse locations that lead to large uncertainties not only with the characterization but also with the interpretation of the sparsely collected information. In DFN approach based on the model described in Ezzedine (2005, 2010), only few details are given here for completeness. The fractures are treated as discs. The density and extensions are difficult to determine independently. An additional parameter called *aperture* is assigned to each disc in the model (Figure 2). The flow is two-dimensional in the fracture plane. The geometrical model assumes that the fractures are finite whose geometric properties, distribution in space, direction and extension can be sampled on the basis of probability distributions deduced from structural observations on the site (Dershowitz et al., 1988).

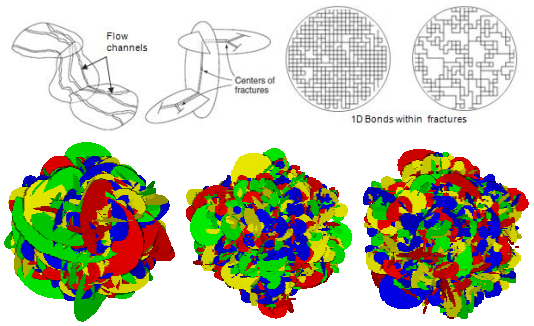

Figure 2: [Top] Example of dimension reduction of a fracture network. Each mother-fracture can be mapped by daughter-fractures. Daughter-fractures are reduced to one dimensional bond.[Bottom]: Example of random simulation of a fractured network.

THE APPROACH: NESTED MONTE CARLO SIMULATION

To summarize the problem in statistical terminology, the geometrical (geological) model is a stochastic one while the flow and thermal problems are solved deterministically within the stochastically generated fractures. However, to solve the mass transport problem, we adopted a stochastic framework, a random walk scheme. Statistically speaking, each SDFN is characterized by: a) a density model; b) an orientation model; c) an aperture model; and d) a radius model. It is worth noting that the number of family of fracture impacts the statistical models of each of the previously listed parameters and the final composition of the fracture network itself.

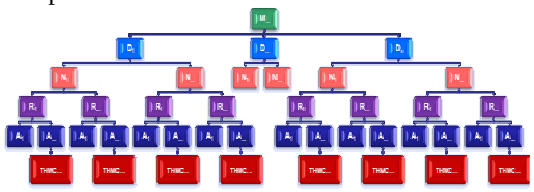

Figure 3: Example of a nested Monte Carlo simulation scheme where each fracture model (M_i: e.g. blak, blue) is characterized by its density (D_i^j), its normal (N_i^j), its radius (R_i^j) and its aperture (A_i^j). The center of each fracture is omitted in the figure but embedded in the density step level.

As one can expect, the space parameters is very large and therefore the number of simulation is exorbitant (Figure 3). Despite that LLNL possesses computer clusters with large number of nodes, a nested Monte Carlo sampling scheme is adopted and the space of parameters is refined as needed based on information-entropy criteria. This enables the current simulation framework to be adopted on a small number of CPUs rather than a brute-force solution. The details of the algorithm are beyond the scope of the present paper; however details can be found in Ezzedine, 2010. In the present paper we focus our efforts on assessing the uncertainty associated with the fracture radius which is by far the most difficult one to ascertain when dealing with sparsely located deep wells.

SIMULATED CASES

In the subsequent sections the flow, heat and mass transport simulations domain has been altered from Ezzedine (2010) to mimic an enhanced geothermal system. The domain is depicted on Figure 4. The goal of the subsequent analyses is to conduct an UQ on the same parameter $<R>/<R_0>$ and its impact on the production temperature profiles as well the mass transport profiles for a tracer test.

The domain of interest is cylinder of 10^3 m radius and 10^3m height with all lateral surfaces are specified 1st type boundary condition set at a pressure of 10m while the injection and extraction wells are set at ¼ distances from the center of the volume (Figure 4).The top and bottom sides of the domain are impervious. The injection and extraction lengths are set to 300m. The injection well is set at a pressure of 1000m. The statistical description of the fracture network is given in Ezzedine (1994 and 2010). The goal is to populate the simulation domain with a 100 SDFN based on the statistical average of the "ground-truth", i.e. the mean radius, <R>, of the fractures is "known" and set to be equal to R_0 (Figure 2).

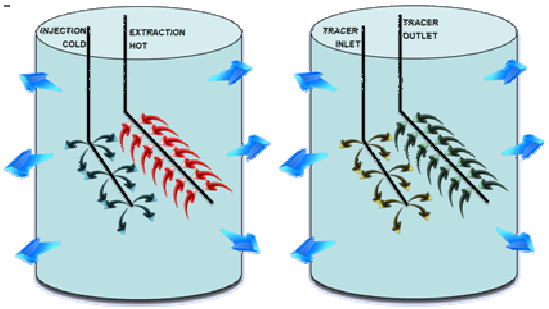

Figure 4: Simulated thermal (left) and transport (right) scenarios: All sides are 1st type boundary conditions (blue arrows); injection well is centered in the domain (black segment) and it is set as a 1st type boundary condition. The injection segment is also a 1st type concentration boundary condition.

Then each of SDFN mean radius <R> is increased or decreased by a factor of 5% such that $<R>/R_0$ spans from 0.5 to 1.5, that is a 50% decrease to 50% increase of R_0. Each 100 SDFN are then re-run 20 times. The 1st and 2nd statistical moments of the in-fluxes (Figure 2) and out-fluxes are calculated. The 1st moment for each $<R>/R_0$ value is then renormalized to the 1st moment correspondent to the "ground-truth" mean flux, i.e. $<q>/q_0$. Similarly the 2nd moment of each $<R>/R_0$ value is also renormalized to the "ground-truth" 2nd moment, i.e. σ^2_q/σ^2_0. Here q_0 and σ^2_0 are the mean and the variance of the "ground-truth" case, respectively (i.e. $<R>=R_0$). The same process is then repeated for the heat and mass at the production well. The 1st and 2nd statistical moments of the temperature and concentration of the tracer are computed for each realization for each variance of $<R>/R_0$. Because we obtained similar conclusions than those previously published, we limit our results here to only heat and mass transport analyses. We refer the readers to Ezzedine (2010) for the flow analyses.

RESULTS & DISCUSSION

Thermal Simulation Analyses

Results of the 1st and 2nd moments are plotted as function of the scaling ratio $<R>/R_0$.

Evolution of temperature as function of time

First and second statistical moments of the evolution of the production temperature as function of time for different scaling ratio $<R>/<R_0> \leq 1$ or ≥ 1 are plotted on Figures 4 and 5, respectively. At a specific time, say 10^6 sec (~12days) a 50% reduction in the radius leads to 25% increase in the mean temperature; while an increase of 50% in the fracture radius leads to a decrease of 35% in production temperature response. This is not surprising because an increase of the radius of the fractures leads to an increase of the fracture connectivity and thus an increase in the number of fractures swept (sampled) by the injected fluid and therefore reducing the mean temperature variability.

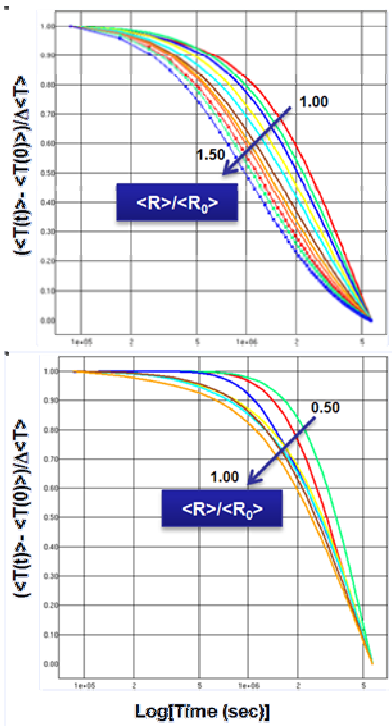

Figure 5: Normalized ensemble-averaged mean temperatures as function of time (sec) for different ratio of $<R>/<R_0>$. [Top] $<R>/<R_0> \leq 1$; [Bottom] $<R>/<R_0> \geq 1$.

On the contrary, at the same specific time ~12days, an increase of 50% fracture radius can lead to doubling the variance of the temperature from the ground-truth case which corresponds to $<R>/<R_0>=1$. It is worth noting, that for $<R>/<R_0> \geq 1$ the 1st and 2nd moments of the temperature after 100MC show a monotonic trends as function of both time and $<R>/<R_0>$; however for $<R>/<R_0> \leq 1$, there is no a specific trends. We believe that 100MCs are not sufficient to fully capture the non-linear behavior of the system.

Behavior of temperature as function of $<R>/<R_0>$

To further our analyses, we have explored the behavior of the ensemble-average production temperatures at different production times (3/4, 2.5 and 4 yrs) for different scaling ratio $<R>/<R_0>$. Figures 6 and 7 depicts the 1st and 2nd statistical moments of the production temperatures and their normalized behavior to the ground-truth case, $<R>/<R_0>$.

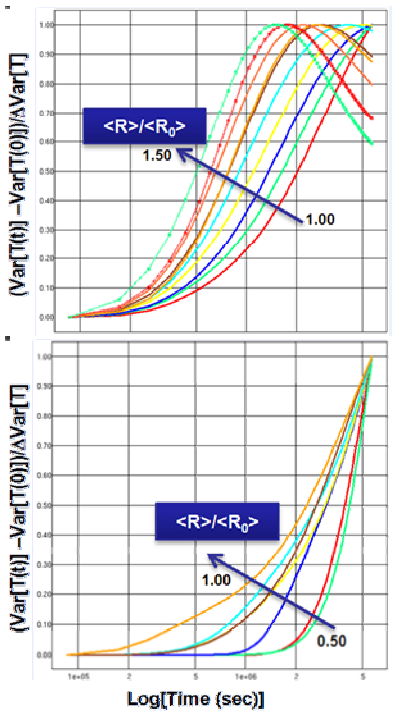

Figure 6: Normalized ensemble-averaged temperature variances as function of time for different ratio of <R>/<R_0>. [Top]<R>/<R_0> ≤1; [Bottom]<R>/<R_0> ≥1.

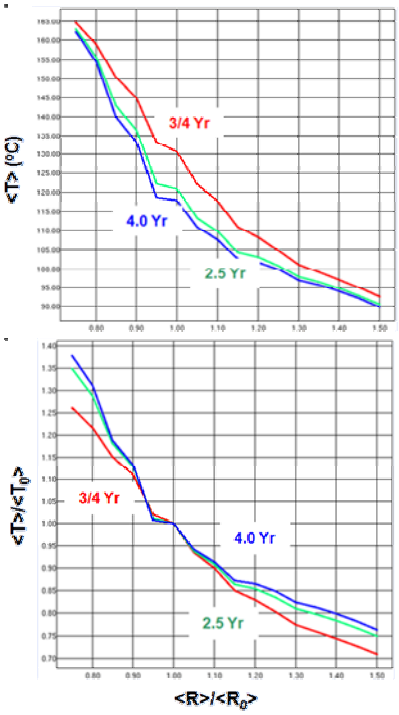

Figure 7: Ensemble-averaged temperature (top) and normalized temperature (bottom) function of different ratio of <R>/<R_0> for different production times (3/4, 2.5 and 4 yrs).

It is worth noting that the 1st and 2nd moments profile at 2.5 and 4.0 years are very similar regardless <R>/<R_0>. Moreover, there is less sensitivity of the average temperature and its variance to the scaling factor when <R>/<R_0> greater than 1, while a larger effect, >greater than 25%, for <R>/<R_0> < 1.

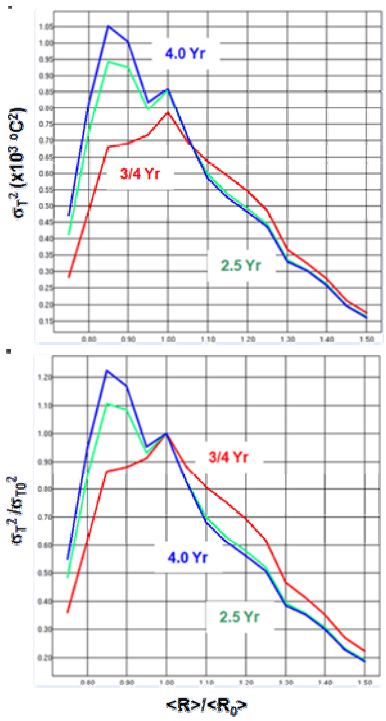

Figure 8: Ensemble-temperature variance (top) and normalized temperature variance (bottom) function of different ratio of <R>/<R_0> for different production times (3/4, 2.5 and 4 yrs).

Tracer simulation results

The domain is depicted on Figure 4. The outer domain is assumed cylindrical. Both upper and bottom surfaces are assumed impervious while the lateral surface is maintained at constant pressure (head) and it is an open boundary condition for mass transport. An initial ½ million particles were injected at the inlet. Particles were transported using a random walk scheme, and recovered at the outlet well. The goal of the subsequent analyses is to conduct an UQ on the same parameter <R>/<R_0> and its impact on the mass transport profiles of a tracer test. Results of the 1st and 2nd moments are plotted as function of the scaling ratio <R>/R_0.

Statistical moments of the tracer

The tracer is assumed conservative, i.e. no sorption, adsorption or chemical reactions are taken place. First statistical moment of the evolution of the tracer concentration as function of time for different scaling ratio <R>/<R_0> ≤ 1 or ≥ 1 are plotted on Figures 9. Similarly to the thermal analyses, the ensemble average of tracer at the outlet , when the scaling factor is less than one, does not have a monotonic behavior with respect to <R>/<R_0>.

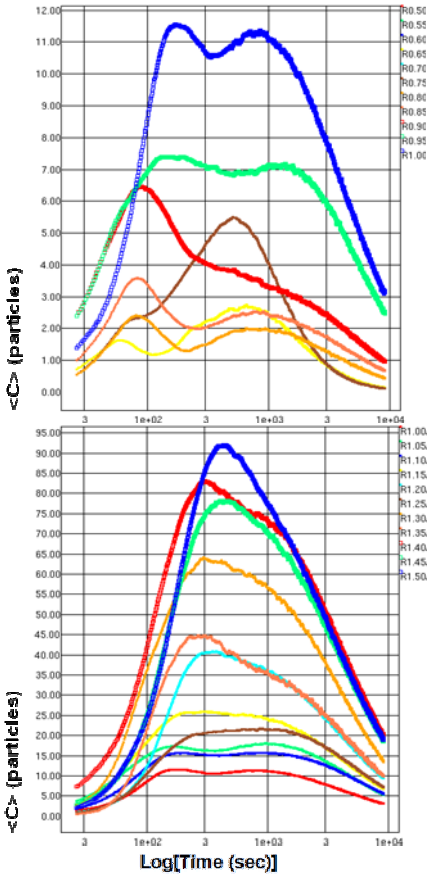

Figure 9: Ensemble average of the concentration (# of particles) of the tracer at the outlet as function of time (# constant time steps) for different (top) $\langle R \rangle / R_0 \rangle \leq 1$, and (bottom) $\langle R \rangle / R_0 \rangle \geq 1$.

This is mainly due to the sparse connectivity between the fractures, the random walk scheme, and, as well the number of Monte Carlo simulations. In fact, the tracer simulation in this case is a 2nd order Monte Carlo simulation, where the 1st (outer) loop is based on the geometry of the fracture network, while the 2nd loop (inner) loop is based on the probabilistic scheme of the random walk, for transporting the particles. At early times, the system has higher entropy while at larger time; a statistical equilibrium can be reached asymptotically. This behavior is more emphasized when $\langle R \rangle / \langle R_0 \rangle > 1$. In the latter case, the connectivity between the fracture increases so is the probability of distribution of the particles within the fracture which leads to a lower statistical entropy; thus a more streamlined behavior, as shown on Figure 9 (bottom).

Second statistical moment of the evolution of the tracer concentration as function of time for different scaling ratio $\langle R \rangle / \langle R_0 \rangle \leq 1$ or ≥ 1 are plotted on Figures 10. Conclusions reached for the 1st moment analyses of the tracer can be extended to the statistical second moment s of the concentration of the tracer.

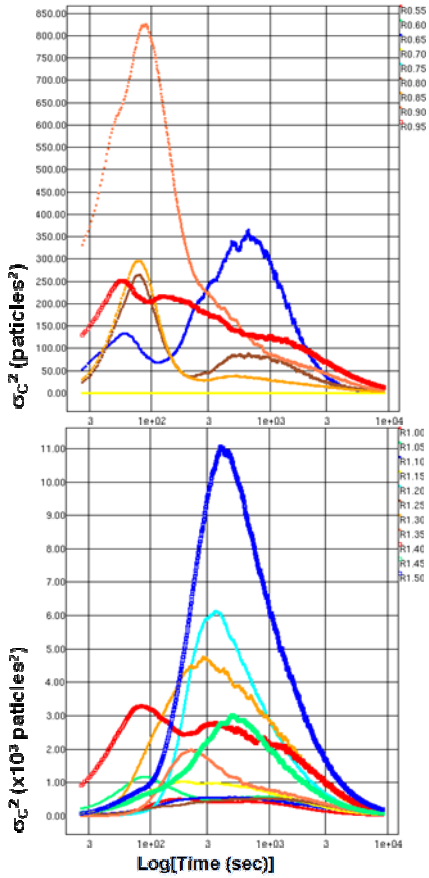

Figure 10: Ensemble variance of the concentration (# of particles^2) of the tracer at the outlet as function of time (# constant time steps) for different (top) $\langle R \rangle / R_0 \rangle \leq 1$, and (bottom) $\langle R \rangle / R_0 \rangle \geq 1$

CONCLUSIONS

We have attempted to address the impact of geological characterization uncertainty on the flow field characteristics using a stochastic discrete fracture network approach. Because the size of the fractures is by far the most difficult parameter to infer from borehole data, we have investigated its uncertainty on the 1st and 2nd moment of the flow (Ezzedine, 2010), heat and mass transport fields. It has been found that under- or over- estimating the mean size (radius) of fractures leads to two distinct responses of the flow, heat and mass fields. Furthermore, the effective hydraulic conductivity, thermal conductivity and dispersion tensors may exhibit anisotropy or isotropy which depends not only on the size of the fractures but also on the boundary conditions of the conceptual model. The anisotropy of tensor is significantly larger when the fracture radius is under-estimated from the ground-truth case. Indeed, the emergence of bimodal

response of the heat and mass transport reflects the co-existence of a fast a slow pathways due to the sparse connectivity of the fracture network, thus the emergence of difference sub-networks (clusters) of fractures. Furthermore, it is worth noting that while the thermal problem is straight forward (stochastic geometry, deterministic physics), the transport problem is a second order probabilistic problem (stochastic geometry and physics) where the non-linear behavior of the system necessitate a larger number of Monte Carlo simulations to ensure convergence.

Despite that geothermal energy is a mature geosciences energy technology and more emerging novel approaches have been proposed, and some have been conceptually analyzed the main problems in EGS remain still the same: i.e. more considerable attention needs to be focused on the fracture characterization.

REFERENCES

Dershowitz W.S. and H.H. Einstein, Characterizing Rock Joint Geometry with joint system models. *Rock Mechanics and Rock Engineering* 21, 21-51, 1988.

DOE, How an Enhanced Geothermal System Works, eere.energy.gov/geothermal/pdfs/egs_basics.pdf, 2011.

Ezzedine, S., 1994, Modeling flow and transport in fractured media using continuum and SDFN approaches. Application to HDR geothermal reservoirs (in French). Ph.D. Thesis, Ecole des Mines de Paris, France, 208p. 1994

Ezzedine S., Stochastic Modeling of Flow and Transport in Porous and Fractured Media. *Chapter 154 in Encyclopedia of Hydrological Sciences*, 34pages, Willey 2005

Ezzedine, S., 2010, Uncertainty Quantification in Enhanced Geothermal Systems using Stochastic Discrete Fractured Network. *35th Stanford Geothermal Workshop, 2010.*

McClure, M. and Horne R., 2010. Modeling Slip during Fluid Injection and Production using Rate/State FrictionMark McClure and Roland Horne. 2010 AGU Fall Meeting, Paper Number H31G-1093

Pruess K, 2006, Enhanced geothermal systems (EGS) using CO2 as working fluid—A novel approach for generating renewable energy with simultaneous sequestration of carbon, *Geothermic* 35(4), 351-367, 2006.

Acknowledgments:

This work performed under the auspices of the U.S. Department of Energy by Lawrence Livermore National Laboratory under Contract DE-AC52-07NA27344. LLNL-PROC-422871-DRAFT.